

Reactions of Butylbenzene Isomers on Zeolite HBeta: Methanol-to-Olefins Hydrocarbon Pool Chemistry and Secondary Reactions of Olefins

Alain Sassi, Mark A. Wildman, and James F. Haw*

Loker Hydrocarbon Research Institute and Department of Chemistry, University of Southern California, University Park, Los Angeles, California 90089-1661

Received: March 27, 2002; In Final Form: June 2, 2002

The reactions of *n*-butylbenzene, isobutylbenzene, *sec*-butylbenzene, and *tert*-butylbenzene on zeolite HBeta ($\text{SiO}_2/\text{Al}_2\text{O}_3 = 150$) were studied at 350 °C using a pulse reactor with GC-MS analysis of product gases. Similar experiments also probed the reactions of butylbenzene isomers with excesses of methanol- ^{13}C . The reactions of *tert*-butylbenzene were also explored as a function of zeolite acid site density and reactant loading. In the absence of secondary reactions such as oligomerization and cracking, olefin product selectivity is governed by the detailed structure of alkyl side chains; for example, *tert*- and isobutylbenzene each yielded isobutene, but *sec*- and *n*-butylbenzene each gave equilibrium mixtures of 1-butene and *cis*- and *trans*-2-butene. The rate of butene elimination from the benzene rings increased with the degree of branching on the carbon α to the aromatic ring as well as the extent of in situ ring methylation by co-fed methanol. In the presence of methanol- ^{13}C , isomerization between 2-butene and isobutene did not occur through a direct pathway; rather skeletal isomerization was observed after chain growth to C_7 or higher olefins followed by cracking. Coking reactions formed volatile alkanes through a mechanism that conserved the carbon skeleton of the precursor olefin. These studies relate to the hydrocarbon pool mechanism of methanol–olefin catalysis (MTO), as well as secondary reactions in MTO chemistry.

Introduction

The long-standing question of which general mechanism explains the catalytic conversion of methanol to hydrocarbons^{1–4} on microporous solid acid catalysts such as HZSM-5 and HSAPO-34 has been answered. The groups of Kolboe^{5–9} and Haw^{10–16} have independently shown, by a variety of methods, that the correct general idea is an indirect mechanism involving a “hydrocarbon pool” of intermediates which is methylated by methanol or dimethyl ether and subsequently eliminates ethylene, propene, and butenes. Using highly pure reagents, we recently demonstrated¹⁷ that methanol and dimethyl ether are unreactive on HZSM-5 and HSAPO-34 in the absence of a hydrocarbon pool, and this finding rules out all direct mechanisms. While a variety of stable cyclic species are capable of serving as reaction centers for methanol catalysis, the most important constituents of the hydrocarbon pool are methylbenzenes. If methylbenzenes can escape from the catalyst (as with unmodified medium pore zeolite HZSM-5), methanol conversion is said to take place under methanol-to-gasoline (MTG) conditions. Alternatively, if the methylbenzenes are trapped in the catalyst (as with the small-pore silico-aluminophosphate HSAPO-34) and secondary reactions of the first-formed olefins are not excessive, the result is methanol-to-olefin (MTO) catalysis. Current research is directed at a more detailed understanding of the structure and function of the hydrocarbon pool. One important question is how does a methylbenzene hydrocarbon pool species extend an alkyl chain that is subsequently eliminated as an olefin? The two possibilities considered are the paring reaction, originally proposed by Sullivan and co-workers,¹⁸ and side-chain methylation, originally proposed by Mole et al.^{19,20} The present contribution does not consider how

the alkyl chain grows, rather it takes the alkyl chain as already formed, and then follows it to products. This study then relates to a second important question, and that is how does the structure of the hydrocarbon pool relate to selectivity for specific olefin products?

Butenes are the smallest olefins to exist in isomeric forms, and so we explored the relationships between the structures of C_4 alkyl chains on alkylbenzene precursors and olefin product distributions. We studied the reactions of all four isomeric butylbenzenes on the large pore zeolite solid acid HBeta at 350 °C, with and without an excess of methanol- ^{13}C . We found that the activity of a butylbenzene isomer for butene elimination was related to the degree of branching on the carbon α to the aromatic ring, and that the structure of the alkyl carbon chain was strongly conserved in the volatile products even for the least reactive isomers. For example, *n*-butylbenzene showed high selectivity for 1-butene and 2-butene, but isobutene was formed preferentially by isobutylbenzene. *cis*- and *trans*-2-Butene and 1-butene were in equilibrium under reaction conditions, but the interconversion of linear butenes and isobutene required chain growth (by oligomerization or reaction with methanol) followed by cracking.^{21,22} Disproportionation of olefins to form alkanes and coke was most significant at higher olefin concentrations and higher zeolite acid site densities. Alkane formation occurred with conservation of carbon skeletal structure; e.g., 2-butene formed *n*-butane rather than isobutane.

Experimental Section

Materials and Reagents. Methanol- ^{13}C (99%) was obtained from Cambridge Isotope Laboratories. *n*-Butylbenzene (99+%), isobutylbenzene (99.8%), *sec*-butylbenzene (99%), *tert*-butylbenzene (98%), and 1,2,3,4-tetrahydronaphthalene (99%) were

* Corresponding author.

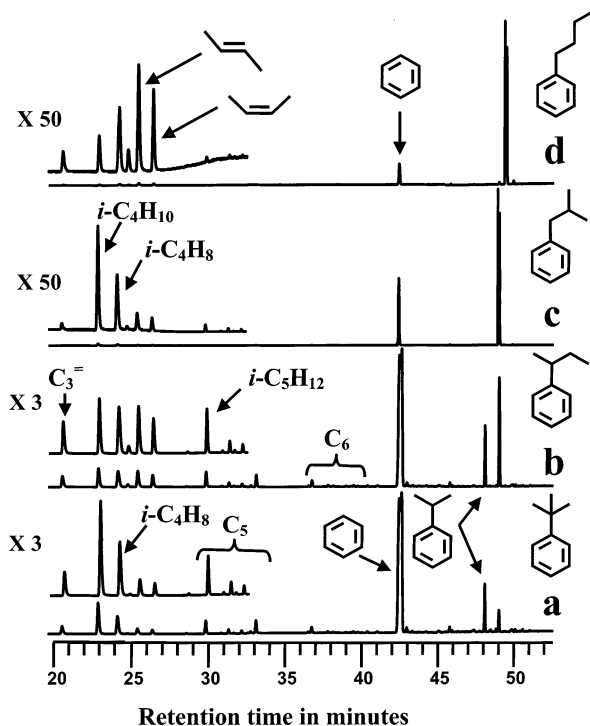


Figure 1. GC-MS total ion chromatograms (Petrocol DH 150 column) from analyses of the volatile products exiting a catalytic reactor (300 mg zeolite HBeta, $\text{SiO}_2/\text{Al}_2\text{O}_3 = 150$, 350°C) sampled 1.5 s following pulsed introduction of 0.123 mmol of various pure butylbenzene compounds. This loading corresponds to two molecules per acid site in the catalyst bed. The short retention time regions (olefins and light alkanes) are scaled as necessary for visualization of these products. (a) *tert*-Butylbenzene was the most reactive isomer and it formed isobutene with high selectivity. (b) *sec*-Butylbenzene was the second-most reactive isomer, and it formed 2-butene with higher selectivity than *tert*-butylbenzene. (c) Isobutylbenzene was less reactive still and formed more isobutene than 2-butene. (d) The reactivity of *n*-butylbenzene (shown) was comparable to that of isobutylbenzene, but 2-butene was formed preferentially in this case.

purchased from Aldrich. Zeolyst International supplied the samples of zeolite HBeta (BEA). These were: CP814E ($\text{SiO}_2/\text{Al}_2\text{O}_3 = 25$), CP811E-75 ($\text{SiO}_2/\text{Al}_2\text{O}_3 = 75$), CP811E-150 ($\text{SiO}_2/\text{Al}_2\text{O}_3 = 150$), and CP811C-300 ($\text{SiO}_2/\text{Al}_2\text{O}_3 = 300$).

Catalysis. We used a benchtop microreactor system¹⁶ for all experiments reported here. All metal components contacting the catalyst, reactants, or products were stainless steel. He (600 sccm) was used as the carrier gas in all experiments. The reactor (5 cm long, 0.65 cm internal diameter) was loaded with 300 mg of fresh HBeta for each experiment which was activated in place immediately prior to use by heating at 500°C for 1 h in flowing helium. All tubing downstream of the chamber was heated. A Valco valve was used to collect a gas sample 1.5 s after each reagent injection.

Gas chromatography (Agilent 6890 Series GC system) with mass spectrometric detection (Agilent 5973) was used to analyze all reaction products. The ionization voltage was 69.9 eV and the source temperature was 240°C . In most of the results shown the products were separated on a 150 m Petrocol DH 150 fused silica capillary column (0.25 mm diameter, 1.0 μm film thickness). A temperature program maintained the oven temperature at 35°C for an initial 25 min followed by a ramp of $20^\circ\text{C}/\text{min}$ to a final temperature of 290°C . The above procedure separated all species of interest with the exception of 1-butene and isobutene, which co-eluted. These compounds have very similar mass spectra; therefore, we repeated the studies of the butylbenzene isomers alone using a second column optimized

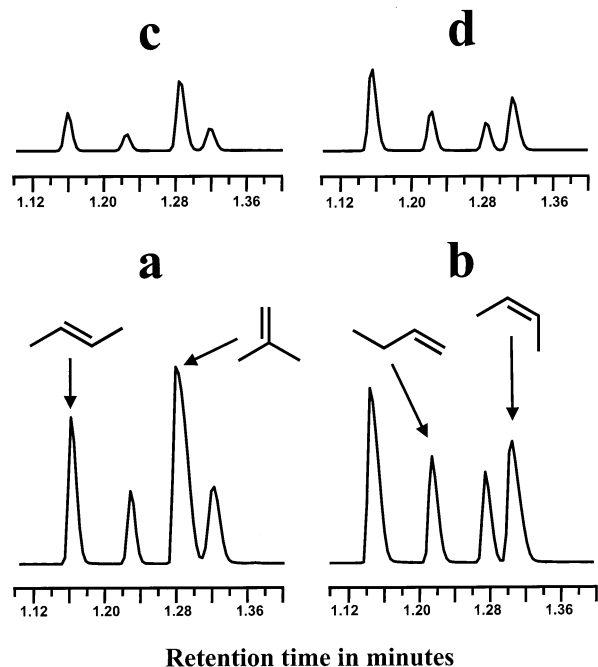


Figure 2. The four experiments in the previous figure were repeated using the alumina column to separate all four butene isomers: (a) *tert*-butylbenzene, (b) *sec*-butylbenzene, (c) isobutylbenzene, and (d) *n*-butylbenzene.

TABLE 1: Enthalpies of Formation in the Gas Phase of Reactants and Products

compounds	$\Delta_f H_{\text{gas}}^\circ$ (kcal/mol)
1-butene	-0.15 ± 0.19
<i>cis</i> -2-butene	-1.83 ± 0.30
<i>trans</i> -2-butene	-2.58 ± 0.24
isobutene	-4.29 ± 0.26
<i>n</i> -butylbenzene	-3.30 ± 0.31
isobutylbenzene	-5.15 ± 0.34
<i>sec</i> -butylbenzene	-4.17 ± 0.33
<i>tert</i> -butylbenzene	-5.42 ± 0.34

for butene separations. This was a 30 m J&W scientific GS alumina column (0.53 mm diameter) operated with a temperature program starting at 120°C and increasing to 200°C with a $20^\circ\text{C}/\text{min}$ ramp. This procedure was used for the chromatograms shown in Figure 2, and it was also used to correct the isobutene yields for 1-butene in the data reported in Table 2.

Results

Butylbenzene Isomers Alone. Figure 1 presents GC-MS total ion chromatograms (Petrocol DH 150 column) characterizing all of the volatile products from the reactions of the four butylbenzene isomers alone on zeolite HBeta ($\text{SiO}_2/\text{Al}_2\text{O}_3 = 150$) catalyst beds at 350°C . In each case 0.123 mmol of butylbenzene (ca. 19 μL) was delivered onto a fresh catalyst bed as a pulse, and the volatile products were sampled 1.5 s later. *tert*-Butylbenzene was the most reactive; 96% conversion was observed in Figure 1a. *sec*-Butylbenzene was slightly less reactive; the conversion in this case was only 87% (Figure 1b). Isobutylbenzene (Figure 1c) and *n*-butylbenzene (Figure 1d) were much less active, with conversions of 13 and 11%, respectively. Cumene (isopropylbenzene) formed as one of the products of either *tert*-butyl- or *sec*-butylbenzene.

Figure 2 reports results from experiments identical to those described above except using the alumina column to obtain separations of all four butene isomers, and these chromatograms most clearly show one of the essential findings of this

TABLE 2: Product Selectivity Data for the Reactions of Butylbenzene Isomers on HBEA at 350 °C

butylbenzene isomer	HBEA (SiO ₂ /Al ₂ O ₃)	butylbenzene conversion (%)	<i>i</i> -C ₄		total C ₄ selectivity	C ₄ H ₈	
			<i>i</i> -C ₄	<i>i</i> -C ₄ + <i>n</i> -C ₄		C ₄ H ₈	C ₄ H ₈ + C ₄ H ₁₀
<i>n</i> -	150	11	0.24		85		0.80
<i>iso</i> -	150	13	0.68		88		0.63
<i>sec</i> -	150	83	0.47		66		0.69
<i>tert</i> -	150	96	0.80		60		0.48
<i>tert</i> -	25	100	0.92		71		0.12
<i>tert</i> -	75	99	0.75		57		0.57
<i>tert</i> -	300	97	0.81		69		0.56
<i>tert</i> -	300 ^a	100	0.77		80		0.95

^a 9.5 mL of *tert*-butylbenzene (one-half of normal) was pulsed on 300 mg of catalyst.

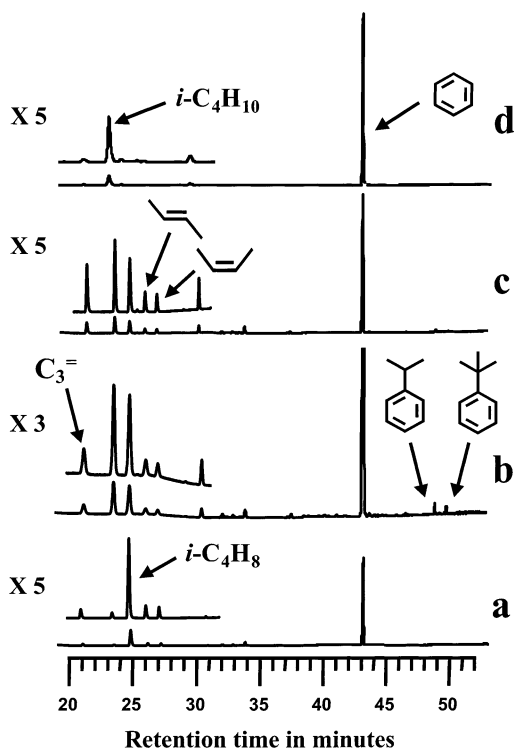


Figure 3. GC-MS total ion chromatograms (Petrocol DH 150 column) from experiments probing the reactions of *tert*-butylbenzene on 300 mg catalyst beds of HBeta at 350 °C under various conditions. (a) 0.123 mmol on a catalyst with SiO₂/Al₂O₃ of 300. Reducing the reactant loading a factor of 2 greatly reduced all secondary reactions and afforded isobutene with a very high selectivity. (b) 0.123 mmol on a catalyst with SiO₂/Al₂O₃ of 300. The olefin yield was higher with the lower acid site density. (c) 0.123 mmol on a catalyst with SiO₂/Al₂O₃ of 75. Coking was also extensive with this acid site density. (d) 0.123 mmol on a catalyst with SiO₂/Al₂O₃ of 25. Extensive coking on this catalyst consumed much of the olefinic products and left isobutane as the predominant C₄ product.

investigation. The olefin isomers formed were largely predetermined by the structure of the alkyl chain on the benzene derivative. Isobutene predominated with *tert*-butylbenzene and isobutylbenzene, but linear butenes were obtained in high yields from *n*-butylbenzene and *sec*-butylbenzene. Table 1 summarizes the gas-phase enthalpies of formation of the four butenes and the four butylbenzenes.²³ The stability order for the butenes is isobutene > *trans*-2-butene > *cis*-2-butene > 1-butene. Independent of the butylbenzene reactant we observed that the ratio of *trans*-2-butene to *cis*-2-butene was always ca. 1.5, and the ratio of 2-butene (*cis*- plus *trans*-) to 1-butene was always ca. 2.5. The fraction of isobutene was strongly dependent on the reactant.

Figure 3 reports GC-MS total ion chromatograms (Petrocol DH 150 column) of the volatile products obtained from *tert*-

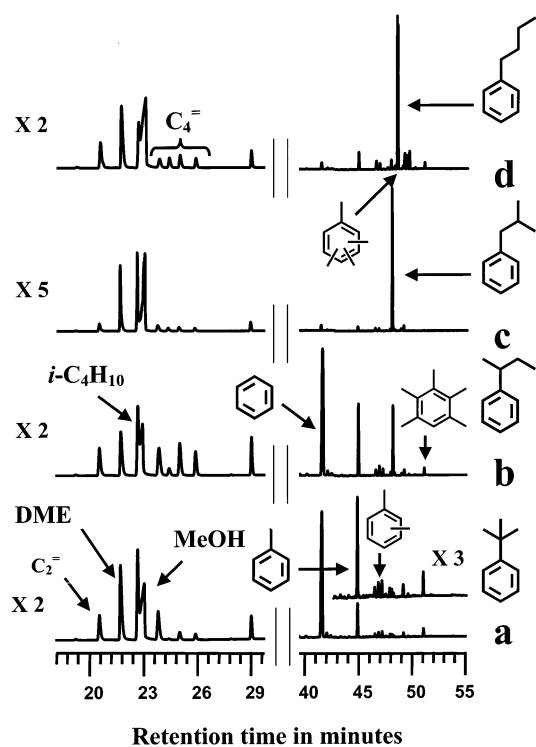


Figure 4. GC-MS total ion chromatograms (Petrocol DH 150 column) from experiments probing the reactions of butylbenzenes with methanol-¹³C. The ratio of methanol-¹³C to butylbenzene was 5:1 (mol:mol). All experiments shown were carried out at 350 °C using HBeta with SiO₂/Al₂O₃ = 150 and gas sampling at 1.5 s. Methanol conversion was in all cases less than quantitative. (a) *tert*-Butylbenzene, (b) *sec*-butylbenzene, (c) isobutylbenzene, (d) *n*-butylbenzene. Selected isotopic distribution data from these experiments are reported in Table 3.

butylbenzene on catalyst beds of HBeta zeolites with various acid site densities. On the highest acid site density studied (SiO₂/Al₂O₃ = 25, Figure 3a) the predominant volatile products were benzene and isobutane. Clearly, this result was dominated by secondary reactions leading to the formation of nonvolatile aromatic coke from some of the primary olefinic products with hydrogen transfer to form isobutane. Product selectivity using a catalyst with SiO₂/Al₂O₃ = 75 (Figure 3b) was very similar to that noted earlier with SiO₂/Al₂O₃ = 150 (Figure 1a). A further modest reduction in secondary reactions occurred when the acid site density was reduced to the lowest value tested (SiO₂/Al₂O₃ = 300, Figure 3c). The largest reduction in alkane formation was achieved when we reduced the *tert*-butylbenzene loading by a factor of 2 on the lowest acid site density catalyst (Figure 3d). In this case, alkane formation was almost completely suppressed.

Table 2 summarizes olefin and alkane product selectivity data from the experiments in Figures 1 and 3. The total C₄ selectivity

TABLE 3: ^{13}C Distribution in the Products Formed by Reaction of a 5:1 Excess of ^{13}C -Methanol and the Butylbenzene Isomers on HBEA ($\text{SiO}_2/\text{Al}_2\text{O}_3 = 150$) at 350 °C

system	C_3H_8	<i>i</i> - C_4H_8	2-butene (<i>cis</i> -)	2-butene (<i>trans</i> -)	<i>i</i> - C_4H_{10}	<i>n</i> - C_4H_{10}	$\Sigma \text{C}_5\text{H}_{10}$	$\Sigma \text{C}_5\text{H}_{12}$	$\Sigma [\text{C}_6\text{H}_{12} + \text{C}_6\text{H}_{14}]$
^{13}C - CH_3OH (excess) + <i>n</i> -butylbenzene									
Total ^{13}C %	18.6	13.4	7.5	7.7	29.2	10	29.2	33.9	38.9
$^{13}\text{C}_0$ (%)	68.3	69.1	81.9	81.5	44.8	81.4	16.9	14.3	10.5
$^{13}\text{C}_1$ (%)	13.7	16.1	10.6	10.6	19.6	2.5	47.5	45.1	20.3
$^{13}\text{C}_2$ (%)	11.7	7.8	4.3	4.5	16.6	12.7	18	15.9	37.7
$^{13}\text{C}_3$ (%)	6.2	4.7	1.9	2.1	12.5	3.3	10	11.3	8.4
$^{13}\text{C}_4$ (%)		1.9	1.3	1.2	6.6	0	5.5	8.4	9.1
$^{13}\text{C}_5$ (%)							2.1	5	7.2
$^{13}\text{C}_6$ (%)									6.7
^{13}C - CH_3OH (excess) + isobutylbenzene									
Total ^{13}C %	16.9	17.4	16.0	15.6	15.8	12.0	33.5	28.5	41.5
$^{13}\text{C}_0$ (%)	63.1	61.3	64.5	63.5	65.2	73.6	13.9	15.4	12.8
$^{13}\text{C}_1$ (%)	24.1	18.4	15.5	20.9	16.7	7.9	39.9	51.9	11.3
$^{13}\text{C}_2$ (%)	11.7	11.4	12.5	7.2	9.8	16.8	22.4	14.2	35.5
$^{13}\text{C}_3$ (%)	1.1	7.1	5.3	5.5	6.8	1.6	14	14.4	19.5
$^{13}\text{C}_4$ (%)		1.8	2.1	2.7	1.6	0	8.3	1.7	7
$^{13}\text{C}_5$ (%)							1.5	2.4	5.1
$^{13}\text{C}_6$ (%)									9.1
^{13}C - CH_3OH (excess) + <i>sec</i> -butylbenzene									
Total ^{13}C %	41.3	22.5	10.5	10.5	33.8	12	33.1	33.0	36.4
$^{13}\text{C}_0$ (%)	25.9	50.1	76.4	76.4	24.3	77.7	13.2	15.4	11.1
$^{13}\text{C}_1$ (%)	35.4	22.4	11.6	11.5	35.3	7.7	40.4	45.6	20.1
$^{13}\text{C}_2$ (%)	27.7	17.1	7.4	7.6	23.3	14.2	23.4	22.9	33.7
$^{13}\text{C}_3$ (%)	11	8.2	3.4	3.4	14.8	3.9	15	13.3	17.6
$^{13}\text{C}_4$ (%)		2.2	1.3	1.3	2.2	0	6.3	6.8	10.8
$^{13}\text{C}_5$ (%)							1.6	1.3	5.3
$^{13}\text{C}_6$ (%)									1.4
^{13}C - CH_3OH (excess) + <i>tert</i> -butylbenzene									
Total ^{13}C %	57.6	33.3	43.5	43.8	28.4	45.1	46.8	46.1	45.6
$^{13}\text{C}_0$ (%)	10.5	38.2	22.2	22.2	50.1	25.2	6.7	2.6	8.0
$^{13}\text{C}_1$ (%)	29.3	19.5	22.2	21.4	13.4	15.5	26.2	35.1	13.5
$^{13}\text{C}_2$ (%)	37.0	19.9	24.9	24.3	16.5	25.0	22.6	20.2	24.9
$^{13}\text{C}_3$ (%)	23.2	15.8	20.7	21.4	12.6	22.9	22.1	20.3	22.3
$^{13}\text{C}_4$ (%)		6.6	10	10.3	7.3	11.5	16.3	15.5	17.3
$^{13}\text{C}_5$ (%)							6.2	6.4	9.1
$^{13}\text{C}_6$ (%)									4.8

and olefin selectivity were inversely correlated with conversion (or loading), reflecting the greater propensity for dimerization and cracking as well as coke formation at higher transient olefin concentrations. 76% of the C_4 products from *n*-butylbenzene were linear (i.e., 1-butene, 2-butene, and *n*-butane), and the balance, 24%, were isobutene and isobutane (Table 2). A higher fraction of branched products was obtained from *sec*-butylbenzene (47%), but branched products clearly predominated with either isobutylbenzene (68%) or *tert*-butylbenzene (80% on the same catalyst used to test the other isomers). The data in Table 2 permit a more quantitative interpretation of the results in Figure 3d. With a reduced loading of *tert*-butylbenzene on the lowest acid site density catalyst, 80% of the volatile products were C_4 and 95% of these were olefins.

Reactions of Methylbenzenes with Methanol. The GC-MS total ion chromatograms (Petrocol DH 150 column) in Figure 4 show that each butylbenzene isomer was more reactive when co-injected with a 5:1 mole ratio of methanol- ^{13}C . For example, the conversion of *n*-butylbenzene increased from 11% to 28% with addition of methanol. With co-added methanol- ^{13}C the aromatic products included not only benzene but also various methylbenzenes with up to five ^{13}C -labeled methyl groups. We also observed some degree of ring methylation with retention of the butyl group; for example, some of the smaller peaks in Figure 4d are due to isomers of methyl- and dimethyl-*n*-butylbenzene.

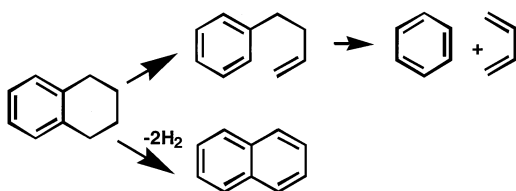
The olefin and alkane products in Figure 4 reflect elimination of the original butyl groups as butenes, reaction of these butenes with methanol- ^{13}C , some additional olefin synthesis from

methanol- ^{13}C on methylbenzene reaction centers, and the consequences of oligomerization and cracking and other secondary reactions. This complex scheme of reactions is reflected in the carbon isotope distributions in the products. These are reported in Table 3 for the four experiments in Figure 4. Distributions are reported for propene, all C_4 products except 1-butene, C_5 olefins (summed over all isomers), C_5 alkanes (summed over all isomers), and the sum of all C_6 olefin and alkane products. Note that the carbon isotope distributions for *cis*- and *trans*-2-butene were invariably identical.

Table 3 contains many numbers, but the essential results can be understood by contrasting *sec*-butylbenzene and *tert*-butylbenzene. For the reactions of *sec*-butylbenzene with methanol- ^{13}C 77% of the 2-butene and 78% of the *n*-butane molecules contained no ^{13}C atoms, but this was true for only 50% of the isobutene and 38% of the isobutane molecules in that same experiment. The isobutene result is an upper limit due to the presence of a small amount of unresolved 1-butene, which would have the same low ^{13}C content as the 2-butene. A reverse ordering was seen in the products from *tert*-butylbenzene and methanol- ^{13}C ; here only 22% of the 2-butene was free of ^{13}C label (25% of *n*-butane), but $^{13}\text{C}_0$ isotopomers predominated for the branched products (isobutene, 38%; isobutane, 50%). In every experiment, the predominant C_5 isotopomers had one ^{13}C —this was true for olefins and alkanes, and the predominant C_6 isotopomers had two ^{13}C atoms. Also, in every case, propene had a higher total ^{13}C content than did the butenes.

Tetrahydronaphthalene. In addition to the four butylbenzene isomers studied above, we also considered 1,2,3,4-tetrahy-

SCHEME 1



dronaphthalene, which could react on zeolite HBeta by at least two routes as described in Scheme 1.

Tetrahydronaphthalene could, in principle, ring open and then eliminate butadiene, which is very reactive on zeolites.²⁴ Alternatively, or in parallel with butadiene elimination and reaction, tetrahydronaphthalene could lose hydrogen and form naphthalene. 1,2,3,4-Tetrahydronaphthalene reacted on HBeta ($\text{SiO}_2/\text{Al}_2\text{O}_3 = 75$) at 350 °C with the evolution of almost no volatile products. We concluded that tetrahydronaphthalene readily forms coke, and we did not study its chemistry any further.

Discussion

Equilibration of Reactants and Products. Table 1 shows the relative stabilities of reactant and product species in the gas phase. *tert*-Butylbenzene is the most stable reactant isomer and this underscores the fact that its greater reactivity has a kinetic origin. There was no evidence of side chain isomerization prior to olefin elimination. A very small amount of *tert*-butylbenzene was seen in some experiments with *sec*-butylbenzene, but this could be accounted for by a sequence of elimination, butene isomerization, and alkylation, in analogy to the route leading to cumene (vide infra).

1-Butene is the least stable butene isomer, and it always formed in lower yield than 2-butene. Previous work has shown that 1-butene isomerizes to 2-butene on acidic zeolites at temperatures below 0 °C without H/D exchange between the olefin and the acid site.²⁵ *n*-Butylbenzene presumably eliminated 1-butene as the primary product and this rapidly equilibrated with 2-butene. The constant relative yields of *cis*- and *trans*-2-butene as well as their identical carbon isotope distributions in all experiments in Table 3 show that these were also in equilibrium with each other.

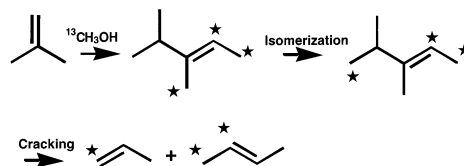
Elimination of Butyl Side Chains from Aromatic Rings.

In a recent investigation we showed that cumene was more reactive than ethylbenzene on zeolite HBeta catalyst.¹⁶ The former eliminated propene and the latter ethylene. Co-injection of methanol-¹³C increased the production of propene-¹³C₀ from cumene and ethylene-¹³C₂ from ethylbenzene by methylating the aromatic rings. Here we observed the activity order *tert*- > *sec*- > *iso*- ≈ *n*- for olefin elimination from butylbenzenes in zeolite HBeta; this is the same ranking that one would anticipate based on analogies to chemistry in acidic solutions. Ring methylation increased the rates of butene elimination, consistent with classical substituent effects in organic chemistry.

Thus, under MTO reaction conditions the structure of the alkyl chain was conserved during olefin elimination. In the absence of secondary reactions, such as dimerization and cracking, the structure of the butene product (linear or branched) was predetermined by the structure of the alkyl chain. This result further supports the connection between the structure of the hydrocarbon pool and olefin product selectivity.

Olefin Chain Growth Followed by Cracking. Butene isomerization on several zeolite catalysts including Ferrierite is believed to occur by dimerization to C₈ olefins that rearrange

SCHEME 2



and crack to form butenes,^{21,22} as well as pentenes plus propene (but not ethylene and hexenes). Dimerization and cracking no doubt also accounts for some of the results reported here.

Table 3 shows that in the presence of methanol-¹³C, butenes undergo chain growth to pentenes and hexenes with (typically), one and two ¹³C atoms, respectively. There is no reason for this process to stop with C₆ olefins; further homologation to C₇ olefins followed by cracking would produce isomeric butenes and propene molecules with mixtures of ¹²C and ¹³C atoms. Scheme 2 illustrated this overall process for the case of isobutene and methanol-¹³C reacting to form 2-butene with two ¹³C atoms and propene with one ¹³C.

This is an important result; it shows that when the concentration of olefins in the catalyst is sufficiently high, methylation of these olefins by methanol/DME competes with methylation of aromatic rings. Aromatic ring methylation leads to ethylene and propene, through previously reported hydrocarbon pool routes. Under the chain growth conditions observed here the olefins must also be considered as reaction centers in the hydrocarbon pool.

cis- and *trans*-2-Butene invariably had identical carbon isotopic distributions, but isobutene had distinct distributions (Table 3). The butane isomers also had distinct carbon isotope distributions that mirrored those of the corresponding olefins. Thus, the formal steps of protonation and hydride transfer to form butanes from butenes occurred without skeletal isomerization.

Cumene Formation. Industrial processes for cumene synthesis co-feed propene and benzene on zeolite HBeta at temperatures somewhat lower than those used in this investigation.^{26,27} Cumene formed here in those experiments where the propene concentration was high; in particular, it formed from *tert*-butylbenzene and *sec*-butylbenzene which gave highest olefin concentrations in the catalyst, and thus propene by way of olefin equilibration. The enthalpy of reaction for making cumene from benzene and propene in the gas phase is -23.76 kcal/mol,²³ and this is slightly more exothermic than the corresponding reactions to form butylbenzenes. For example, the formation of *tert*-butylbenzene from isobutene and benzene has a very slightly less favorable ΔH of -20.95 kcal/mol. Thus under conditions in which secondary reactions lead to comparable concentrations of propene and isobutene in the catalyst, cumene can be seen under conditions where the equilibrium concentration of *tert*-butylbenzene is much lower. Cumene formation underscores the fact that benzene de-alkylation is reversible in these experiments.

Conclusions

Under MTO reaction conditions in zeolite HBeta C₄ side chains are eliminated from benzene rings with retention of carbon skeletal structure, and branching on the carbon α to the aromatic ring increases the rate of elimination. With a high concentration of butenes in the catalyst the rate at which methanol and dimethyl ether reacted with olefins was competitive with the rate of benzene ring methylation. Thus, the olefins functioned as components of the hydrocarbon pool. When the

butylbenzenes were reacted with methanol, butene isomerization was observed and it occurred by chain growth followed by cracking. In the absence of methanol, butene isomerization apparently occurred by oligomerization and cracking, as observed in previous work, and it was suppressed by reducing the amount of feed pulsed onto the catalyst. Disproportionation of butenes to form butanes and coke was most rapid on catalysts with a higher acid site density and it occurred with conservation of the carbon skeletal structure.

Acknowledgment. This work was supported by the National Science Foundation (CHE-9996109) and the U.S. Department of Energy (DOE) Office of Basic Energy Sciences (BES) (Grant No. DE-FG03-93ER14354). Alain Sassi acknowledges the Deutsche Forschungsgemeinschaft (DFG) for their financial support.

References and Notes

- (1) Chang, C. D. *Catal. Rev.* **1983**, *25*, 1–118.
- (2) Stöcker, M. *Microporous Mesoporous Mater.* **1999**, *29*, 3–48.
- (3) Keil, F. J. *Microporous Mesoporous Mater.* **1999**, *29*, 49–66.
- (4) Chang, C. D. Shape-selective catalysis: chemicals synthesis and hydrocarbon processing. Song, C., Garces, J. M., Sugi, Y., Ed.; ACS Symposium Series 738, Washington DC, 2000.
- (5) Dahl, I. M.; Kolboe, S. *J. Catal.* **1996**, *161*, 304–309.
- (6) Dahl, I. M.; Kolboe, S. *J. Catal.* **1994**, *149*, 458–464.
- (7) Mikkelsen, O.; Ronning, P. O.; Kolboe, S. *Microporous Mesoporous Mater.* **2000**, *40*, 95–113.
- (8) Arstad, B.; Kolboe, S. *Catal. Lett.* **2001**, *71*, 209–212.
- (9) Arstad, B.; Kolboe, S. *J. Am. Chem. Soc.* **2001**, *123*, 8137–8138.
- (10) Goguen, P. W.; Xu, T.; Barich, D. H.; Skloss, T. W.; Song, W.; Wang, Z.; Nicholas, J. B.; Haw, J. F. *J. Am. Chem. Soc.* **1998**, *120*, 2651–2652.
- (11) Haw, J. F.; Nicholas, J. B.; Song, W.; Deng, F.; Wang, Z.; Heneghan, C. S. *J. Am. Chem. Soc.* **2000**, *122*, 4763–4775.
- (12) Song, W.; Haw, J. F.; Nicholas, J. B.; Heneghan, K. *J. Am. Chem. Soc.* **2000**, *122*, 10726–10727.
- (13) Song, W.; Fu, H.; Haw, J. F. *J. Am. Chem. Soc.* **2001**, *123*, 4749–4754.
- (14) Song, W.; Fu, H.; Haw, J. F. *J. Phys. Chem. B* **2001**, *105*, 12839–12843.
- (15) Fu, H.; Song, W.; Haw, J. F. *Catal. Lett.* **2001**, *76*, 89–94.
- (16) Sassi, A.; Wildman, M.; Ahn, H. J.; Prasad, P.; Nicholas, J. B.; Haw, J. F. *J. Phys. Chem. B* **2002**, *106*, 2294–2303.
- (17) Song, W.; Marcus, D. M.; Fu, H.; Ehresmann, J. O.; Haw, J. F. *J. Am. Chem. Soc.* **2002**, *124*, Web Release in March, 2002.
- (18) Sullivan, R. F.; Egan, C. J.; Langlois, G. E.; Sieg, R. P. *J. Am. Chem. Soc.* **1961**, *83*, 1156–1160.
- (19) Mole, T.; Whiteside, J. A.; Seddon, D. *J. Catal.* **1983**, *82*, 261–266.
- (20) Mole, T.; Bett, G.; Seddon, D. *J. Catal.* **1983**, *84*, 435–445.
- (21) Bearez, C.; Chevalier, F.; Guisnet, M. *React. Kinet. Catal. Lett.* **1983**, *22*, 405–411.
- (22) Guisnet, M.; Andy, P.; Gnep, N. S.; Benazzi, E.; Travers, C. *J. Catal.* **1996**, *158*, 551–560.
- (23) NIST Chemistry WebBook (<http://webbook.nist.gov/chemistry/>).
- (24) Richardson, B. R.; Lazo, N. D.; Schettler, P. D.; White, J. L.; Haw, J. F. *J. Am. Chem. Soc.* **1990**, *112*, 2886–2891.
- (25) Kondo, J. N.; Domen, K.; Wakabayashi, F. *Microporous Mesoporous Mater.* **1998**, *21*, 429–437.
- (26) Ward, D. J. U. S. Patent 4,008,290, 1977.
- (27) Smith, L. A., Jr.; Arganbright R. P.; Hearn D. U.S. Patent 5,055,627, 1991.